Unique Loss Characteristics in TE_01 Modes of Conventional Photonic Bandgap Fibers

Unique Loss Characteristics in TE_{01} Modes of Conventional Photonic Bandgap Fibers

HIROKAZU KUBOTA[1,*], NOBUAKI KOSAKE[1], YUJI MIYOSHI[1], AND MASAHARU OHASHI[1]

[1] Graduate School of Engineering, Osaka Prefecture University, 1-1 Gakuencho, Naka-ku, Sakai-shi, 599-8531
[*] Corresponding author: kubota@eis.osakafu-u.ac.jp

Compiled April 10, 2018

We report modeling that demonstrates reduction of transmission loss and broadening of the bandwidth of a conventional hollow-core photonic bandgap fiber. Numerical investigation reveals that transmission loss of the high order TE_{01} mode is lower than that of the fundamental HE_{11} mode in fibers with thick cladding walls. By comparing dispersion curves of photonic bandgap fibers with different core-wall thicknesses, we show that the TE_{01} mode has weaker coupling strength to a surface mode than the HE_{11} mode does. This result opens way for wider transmission band and lower transmission loss in photonic bandgap fibers that are subject to the detrimental effects of surface modes.

OCIS codes: (060.4005) Microstructured fibers, (060.5295) Photonic crystal fibers.

http://dx.doi.org/10.1364/ao.XX.XXXXXX

1. INTRODUCTION

Hollow core fibers have a range of useful properties compared to solid-core optical fiber. These include low nonlinearity, low latency, low group velocity dispersion (GVD), low propagation loss and the ability to guide over a wide spectral region. Photonic bandgap fiber (PBF) is a well known type of hollow core fiber made of an air core surrounded by a photonic crystal cladding, which comprises a periodic array of air holes in transparent dielectric material, surrounding the core [1]. The loss mechanisms of the PBF include confinement loss, scattering at the core-cladding boundary, and mode coupling between core modes and cladding modes, in addition to material absorption [2]. Reducing the surface roughness of the core- cladding boundary and enlargement of the propagating mode area have been employed to make low-loss [3].

Reducing the coupling between the core mode and cladding modes such as surface modes has been a challenging problem in the pursuit of low-loss hollow core fibers. Control of the mode coupling between the core mode and surface modes has been used to achieve low-loss, wide bandwidth PBFs [4–9]. In a conventional PBF, reducing the thickness of the core-wall has been shown to reduce of the surface mode in the tube that surrounds the air core [6]. Anti-resonant hollow core fiber generated much interest in 2010's because of the simplicity of the structure and no requirement for a periodic cladding structure [7, 8]. In the anti-resonant structure, the surface normal vector of the core boundary is oppositely directed to the surface normal vector of the electric field distribution of the core modes which inhibits coupling between the core modes and the cladding modes.

Most loss analyses in the literature have been focused on the fundamental mode because high order modes tend to have a higher transmission loss. In this paper, we numerically investigate mode profiles, dispersion curves, and transmission losses of the high order modes of TE_{01}, TM_{01}, and HE_{21} mode of the conventional hollow-core PBF, which referred as LP_{11} mode in the weak guidance approximation. We find that one of the high order modes of the PBF, namely TE_{01}, shows comparably low transmission loss to the fundamental HE_{11} mode, and in some cases, even lower. We ascribe the lower loss of the TE_{01} to its weaker coupling strength to a surface mode compared with that of the HE_{11} mode.

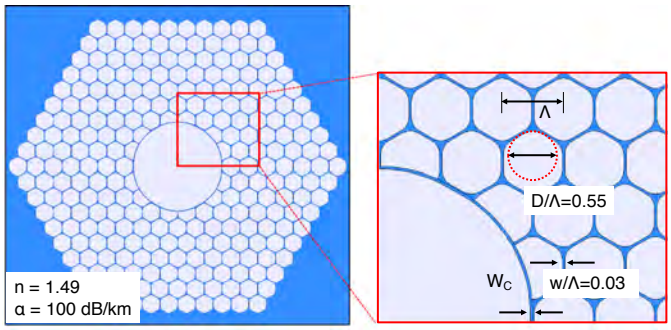

Fig. 1. Cross-sectional view of the hollow-core PBF model with a 7-ring conventional photonic crystal cladding.

2. FIBER MODEL

Figure 1 shows an cross-sectional view of the hollow-core PBF used in our calculations. The parameters were normalized with respect to the center-to-center distance between the two adjacent air holes, Λ. The cladding of our PBF has a photonic crystal (PC) structure, which comprises 7 rings of hexagonal air holes with rounded internal vertices. The PC is described by two parameters [10], the thickness of cladding struts, w, and the

diameter of curvature at the vertices, D. We set w/Λ = 0.03 and D/Λ = 0.55. The central 19 cells were removed to make a fiber core structure and we assume that the cladding struts facing to the core forms a ring shaped "core-wall". We calculated two cases of the core-wall thickness W_C. One had a thin core-wall (W_C= 0.01 Λ), which is known to reduce surface mode [3], and the other had a moderately thicker core-wall (W_C/Λ= 0.03) which allows core modes to couple to surface modes.

A full-vector finite element method was used to calculate effective indices and mode profiles of the PBF. The refractive index n and absorption coefficient α of the material were set at 1.49 and 100 dB/km, respectively, assuming the material was PMMA at a wavelength around 650 nm. The material dispersion was estimated by interpolating a measured refractive index reported in [11]. Using the above parameter values, a photonic bandgap appears at a wavelength range from λ = 590 to 660 nm when the Λ was 1.34 μm.

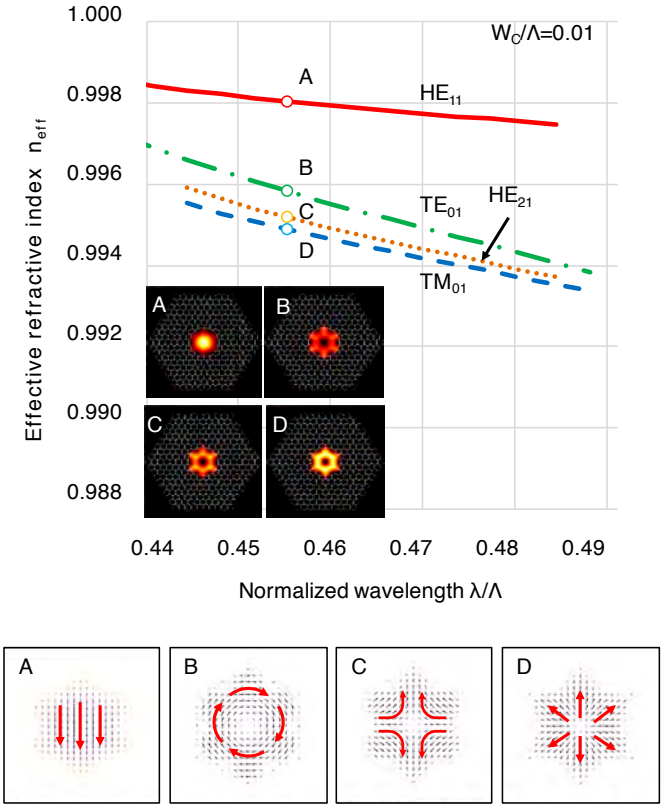

Fig. 2. Dispersion curves of the PBF with a core-wall thickness of W_C= 0.01 Λ of a HE_{11} (red, solid), TE_{01} (green, dash-dotted), HE_{21} (orange, dotted) and TM_{01} (blue, dashed) modes. The intensity profiles of each mode are shown in the inset. Corresponding vector field plot is shown in the bottom and schematic direction of E-field is overlaid on each vector plot.

3. DISPERSION CURVE AND TRANSMISSION LOSS

At first, we calculated a model with a thin core wall of W_C/Λ= 0.01. We choose the thickness of which a surface mode was not observed. Figure 2 shows calculated dispersion curves of a fundamental and 1st high order mode group. Typical intensity profiles of each mode at λ/Λ=0.455, indicated by open circles on the dispersion curves, are also shown in the inset.

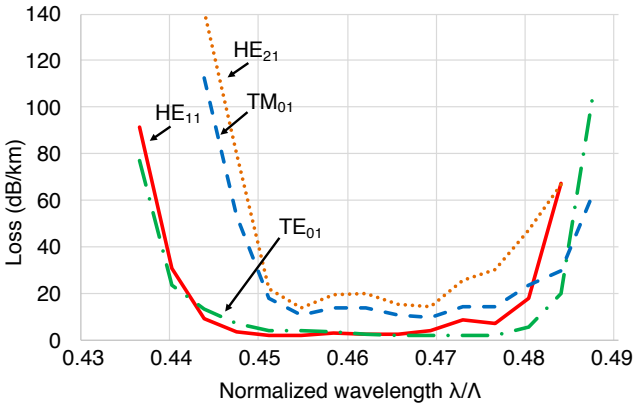

Fig. 3. Transmission loss of the PBF with a core-wall thickness of W_C= 0.01 Λ of a HE_{11} (red, solid), TE_{01} (green, dash-dotted), HE_{21} (orange, dotted) and TM_{01} (blue, dashed) modes.

We found two circular shaped modes, which were a fundamental mode of a degeneracy of two, and four doughnut shaped modes, which we identified asTE_{01}, 2 degenerate HE_{21}, and TM_{01} modes. The lower images are the corresponding electric fields plots. Schematic direction of the electric field is overlaid on each image as red arrows. We checked their electric field vectors to distinguish for each mode a dispersion curve. These four doughnut shaped modes are classified as a LP_{11} mode in the weak guidance approximation, though the dispersion curves and the electric fields indicate the weak guidance approximation does not hold in this hollow-core PBF[12]. All the dispersion curve for HE_{11} (red, solid line), TE_{01} (green, dash-dotted), HE_{21} (orange, dotted) and TM_{01} (blue, dashed) modes were almost straight. The intensity profiles show the modes were well confined in the core region and have no surface modes.

Figure 3 shows calculated transmission losses of a fundamental and 1st high order mode group. The transmission loss of the HE_{11} mode was flat over the bandgap region. The transmission loss increase was not observed within the bandgap region. As expected, the higher order modes of HE_{21} mode (orange, dotted line) and the TM_{01} mode (blue, dashed line) exhibit higher loss than the fundamental HE_{11} mode. Unlike these modes, the TE_{01} mode (green, dash-dotted line) showed transmission loss as low as that of a HE_{11} mode even though TE_{01}, HE_{21} and TM_{01} modes are classified as LP_{11} mode group in the weak guidance approximation. The low loss regions for the HE_{21} and TM_{01} modes were shifted to longer wavelengths because the respective band edges of their photonic bandgaps shift to longer wavelength region for their lower effective index. Bandwidth of the TE_{01} low-loss wavelength region was also comparable to that of a HE_{11} mode. Neither the dispersion curve nor the transmission loss curves show any evidence of coupling of core modes to surface modes.

Next, we calculated a fiber model that the core-wall has same thickness as the cladding struts, W_C= 0.03 Λ. Figure 4 shows dispersion curves, transmission losses and vector plots of the calculated modes. In the figure, plots corresponding to the HE_{21} mode were omitted for simplicity. Thin black lines indicate expected dispersion curve of core mode (solid line) and surface modes (dotted lines) if there were no mode coupling. The thin dotted lines at the left most of HE_{11} mode and right most of TM_{01} are derived from asymptotic line of corresponding curves.

Mode profiles and dispersion curves became complicated due to mode coupling between the core modes and surface modes. The dispersion curves of the HE_{11} mode (red, solid lines) were a pair of anti-coupling lines. Both of the lines shows wavy shape, indicating that the HE_{11} mode couples with more than one surface modes. We found slope of the core mode without mode coupling is the same as the slope of the HE_{11} mode in thin core wall case.

The dispersion curve of the TM_{01} mode (blue, dashed line) has convex shape and was 4 times steeper than that in thin core wall case. This indicates that the blue dashed line was coupled mode of TM_{01} mode and a surface mode although we cannot find the counterpart of the blue dashed line. A thin dotted line aside the blue dashed line indicates a dispersion curve of the surface mode. Its slope is about the same as the slope of the surface mode that couples with the HE_{11} mode, it supports above assumption that the thin dotted line is a dispersion curve of the surface mode coupled with the TM_{01} mode. The green dash-dotted line shows a dispersion curve of the TE_{01} mode. The slope of the curve remains the same as that in thin core wall case. This means that the mode coupling between the TE_{01} mode and surface mode is very weak.

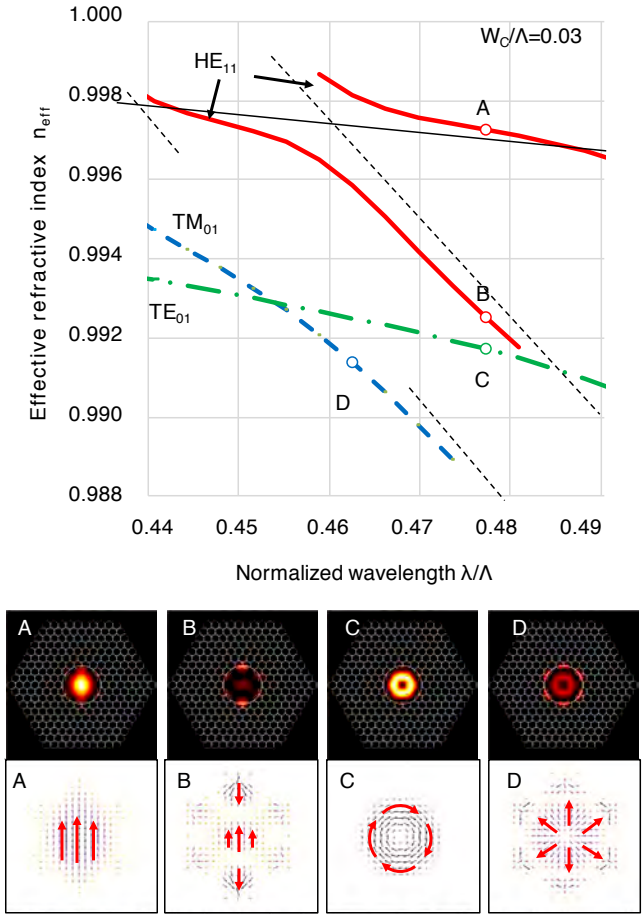

Fig. 4. Dispersion curves of the PBF with a core-wall of W_c= 0.03Λ. of a HE_{11} (red, solid), TE_{01} (green, dash-dotted), and TM_{01} (blue, dashed) modes. The intensity and the vector field plot is shown in the bottom. Schematic direction of E-field is overlaid on each vector plot. Plots corresponding to HE_{21} mode are omitted for simplicity.

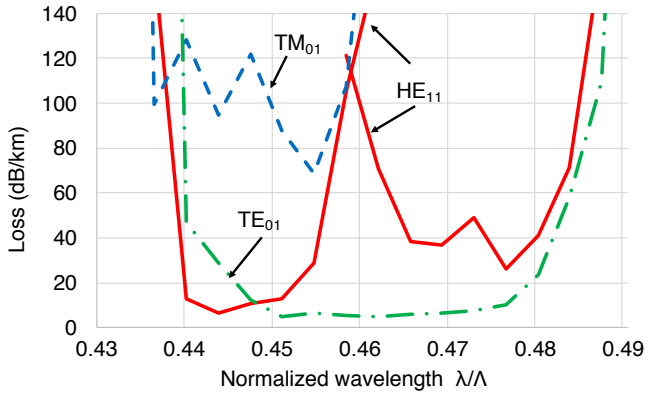

Fig. 5. Transmission loss of the PBF with a core-wall of W_c= 0.03Λ. of a HE_{11} (red, solid), TE_{01} (green, dash-dotted), and TM_{01} (blue, dashed) modes.

The bottom of Fig. 4 shows the intensity profiles and the vector plot of the typical electric field profiles of each mode at points marked by open circles on the respective dispersion curves; A and B are the coupled mode of HE_{11} mode and surface mode, of core mode dominant case and surface mode dominant case, C is the TE_{01} mode, which shows very little coupling with a surface mode, and D is the TM_{01} mode, which shows strong coupling with a surface mode. The amount of mode coupling shown in these vector plots are consistent to the mode coupling strength understood by the dispersion curves.

Figure 5 shows transmission losses of HE_{11} (red, solid), TE_{01} (green, dash-dotted), and TM_{01} (blue, dashed) modes. Transmission loss increases at the band edges of the photonic bandgap and where a surface mode is dominant because the surface mode has large loss. Thus each line has a U-shape. The lines were plotted for each dispersion curve, i.e., two lines were plotted for the HE_{11} mode. The transmission loss of the HE_{11} mode follows lower value of the two U-shaped lines, consequently it becomes W-shaped.

The TM_{01} mode had a low loss region only a half of the bandgap area. The loss of the counter part of the blue dashed line may very high. The transmission loss of the TE_{01} mode remained low over the bandgap region. This also indicates weak mode coupling between TE_{01} and a surface mode. The lowest transmission loss of the TE_{01} mode was comparable to that of the HE_{11} mode, in addition, weak mode coupling to the surface modes prevent loss increase within the bandgap wavelengths.

There are several reports of the TE_{01} mode generation in few-mode fibers[13, 14], but the TE_{01} mode generation technique suitable for optical communication is an open issue.

4. CONCLUSION

We numerically investigated mode profile, dispersion curves, and transmission loss of the high order modes of the conventional hollow-core PBF. We found that one of a high order mode, TE_{01} mode, of the PBF had comparably low transmission loss to that of the fundamental HE_{11} mode, while other high order modes showed larger transmission loss than the fundamental mode. The mode coupling between TE_{01} mode and the surface mode was weak. The weak mode coupling eliminates restriction of the transmission band due to the surface mode even when the surface mode exists in a relatively thick core-wall. When

the TE_{01} mode can be launched into a PBF, wide-band low-loss transmission may be possible with a conventional PBF.

REFERENCES

1. T. A. Birks, P. J. Roberts, P. S. J. Russell, D. M. Atkin, and T. J. Shepherd, Electron. Lett. **31**, 1941 (1995).
2. J. A. West, C. M. Smith, N. F. Borrelli, D. C. Allan, and K. W. Koch, Opt. Express **12**, 1485 (2004).
3. P. J. Roberts, D. P. Williams, B. J. Mangan, H. Sabert, F. Couny, W. J. Wadsworth, T. A. Birks, J. C. Knight, and P. S. Russell, Opt. Express **13**, 8277 (2005).
4. K. Saitoh, N. A. Mortensen, and M. Koshiba, Opt. Express **12**, 394 (2004).
5. R. Amezcua-Correa, N. G. R. Broderick, M. N. Petrovich, F. Poletti, and D. J. Richardson, Opt. Express **14**, 7974 (2006).
6. N. V. Wheeler, M. N. Petrovich, R. Slavik, N. Baddela, E. Numkam, J. R. Hayes, D. R. Gray, F. Poletti, and D. J. Richardson, "Wide-bandwidth, low-loss, 19-cell hollow core photonic band gap fiber and its potential for low latency data transmission," in "OFC/NFOEC," (2012), pp. 1–3.
7. Y. Y. Wang, N. V. Wheeler, F. Couny, P. J. Roberts, and F. Benabid, Opt. Lett. **36**, 669 (2011).
8. A. D. Pryamikov, A. S. Biriukov, A. F. Kosolapov, V. G. Plotnichenko, S. L. Semjonov, and E. M. Dianov, Opt. Express **19**, 1441 (2011).
9. M. Michieletto, J. K. Lyngs¥o, J. L¥aegsgaard, and O. Bang, Opt. Express **22**, 23324 (2014).
10. N. A. Mortensen and M. D. Nielsen, Opt. Lett. **29**, 349 (2004).
11. Shimazu, "Precision Refractometer," https://www.shimadzu.co.jp/products/opt/products/ref/ref-app01.html.
12. K. Z. Aghaie, V. Dangui, M. J. F. Digonnet, S. Fan, and G. S. Kino, IEEE J. Quantum Electron. **45**, 1192 (2009).
13. G. Volpe and D. Petrov, Opt. Commun. **237**, 89 (2004).
14. Z. Fang, Y. Yao, K. Xia, M. Kang, K. ichi Ueda, and J. Li, Opt. Commun. **294**, 177 (2013).

FULL REFERENCES

1. T. A. Birks, P. J. Roberts, P. S. J. Russell, D. M. Atkin, and T. J. Shepherd, "Full 2-D photonic bandgaps in silica/air structures," Electron. Lett. **31**, 1941–1943 (1995).
2. J. A. West, C. M. Smith, N. F. Borrelli, D. C. Allan, and K. W. Koch, "Surface modes in air-core photonic band-gap fibers," Opt. Express **12**, 1485–1496 (2004).
3. P. J. Roberts, D. P. Williams, B. J. Mangan, H. Sabert, F. Couny, W. J. Wadsworth, T. A. Birks, J. C. Knight, and P. S. Russell, "Realizing low loss air core photonic crystal fibers by exploiting an antiresonant core surround," Opt. Express **13**, 8277–8285 (2005).
4. K. Saitoh, N. A. Mortensen, and M. Koshiba, "Air-core photonic band-gap fibers: the impact of surface modes," Opt. Express **12**, 394–400 (2004).
5. R. Amezcua-Correa, N. G. R. Broderick, M. N. Petrovich, F. Poletti, and D. J. Richardson, "Optimizing the usable bandwidth and loss through core design in realistic hollow-core photonic bandgap fibers," Opt. Express **14**, 7974–7985 (2006).
6. N. V. Wheeler, M. N. Petrovich, R. Slavik, N. Baddela, E. Numkam, J. R. Hayes, D. R. Gray, F. Poletti, and D. J. Richardson, "Wide-bandwidth, low-loss, 19-cell hollow core photonic band gap fiber and its potential for low latency data transmission," in "OFC/NFOEC," (2012), pp. 1–3.
7. Y. Y. Wang, N. V. Wheeler, F. Couny, P. J. Roberts, and F. Benabid, "Low loss broadband transmission in hypocycloid-core kagome hollow-core photonic crystal fiber," Opt. Lett. **36**, 669–671 (2011).
8. A. D. Pryamikov, A. S. Biriukov, A. F. Kosolapov, V. G. Plotnichenko, S. L. Semjonov, and E. M. Dianov, "Demonstration of a waveguide regime for a silica hollow - core microstructured optical fiber with a negative curvature of the core boundary in the spectral region > 3.5 μm," Opt. Express **19**, 1441–1448 (2011).
9. M. Michieletto, J. K. Lyngs¥o, J. L¥aegsgaard, and O. Bang, "Cladding defects in hollow core fibers for surface mode suppression and improved birefringence," Opt. Express **22**, 23324–23332 (2014).
10. N. A. Mortensen and M. D. Nielsen, "Modeling of realistic cladding structures for air-core photonic bandgap fibers," Opt. Lett. **29**, 349–351 (2004).
11. Shimazu, "Precision Refractometer," https://www.shimadzu.co.jp/products/opt/products/ref/ref-app01.html.
12. K. Z. Aghaie, V. Dangui, M. J. F. Digonnet, S. Fan, and G. S. Kino, "Classification of the core modes of hollow-core photonic-bandgap fibers," IEEE J. Quantum Electron. **45**, 1192–1200 (2009).
13. G. Volpe and D. Petrov, "Generation of cylindrical vector beams with few-mode fibers excited by laguerre–gaussian beams," Opt. Commun. **237**, 89 – 95 (2004).
14. Z. Fang, Y. Yao, K. Xia, M. Kang, K. ichi Ueda, and J. Li, "Vector mode excitation in few-mode fiber by controlling incident polarization," Opt. Commun. **294**, 177 – 181 (2013).